IEEE Access
Multidisciplinary | Rapid Review | Open Access Journal

Received 31 May 2023, accepted 13 June 2023, date of publication 16 June 2023, date of current version 22 June 2023.

Digital Object Identifier 10.1109/ACCESS.2023.3287140

RESEARCH ARTICLE

Robust Localization Method Based on Non-Parametric Probability Density Estimation

CHEE-HYUN PARK AND JOON-HYUK CHANG, (Senior Member, IEEE)
Department of Electronics Engineering, Hanyang University, Seoul 133-791, South Korea

Corresponding author: Joon-Hyuk Chang (jchang@hanyang.ac.kr)

This work was supported by Institute of Information & communications Technology Planning & Evaluation (IITP) grant funded by the Korea Government [Ministry of Science and Information and Communications Technology (MSIT)] (No.2021-0-00456, Development of Ultra-high Speech Quality Technology for Remote Multi-speaker Conference System).

ABSTRACT This paper presents robust localization techniques that calculate location using distance observations. In enclosed and heavily populated urban environments, the positive measurement bias introduced by a non-line-of-sight signal can have a considerable adverse impact on estimation performance. Therefore, to mitigate the detrimental effects of the multipath effect caused by the non-line-of-sight signal, robust localization techniques are considered. In particular, the k-nearest neighbor (KNN)-based and orthogonal series (OSERIES)-based localization approaches are proposed. The difference from conventional probability density estimation (PDF) estimation methods is that the proposed methods use the first-peak information of the estimated PDF to obtain the actual distance information, not just the PDF shape estimation. More specifically, the proposed methods use the mean calculated from observations selected by statistical testing because the mean estimate generally outperforms the mode estimate. In addition, the Rao test in the context of the two-mode Gaussian mixture model (GMM) is demonstrated to be uniformly most powerful (UMP) test. Furthermore, the conditional variance of the range measurement is derived. Also, the proposed techniques outperforms that of competing algorithms in terms of localization accuracy.

INDEX TERMS First peak, Gaussian mixture model, k-nearest neighbor, localization, non-line-of-sight, orthogonal series, probability density function, weighted least squares.

I. INTRODUCTION

In sensor node positioning, the time difference of arrival (TDOA), time of arrival (TOA), received signal strength (RSS), and angle of arrival (AOA) are measurements utilized to determine the position of the target node. Numerous research fields, including mobile communications, telecommunications, and the Internet of Things, depend on location awareness. In instances involving line-of-sight (LOS), there is no blocking or impediment. However, non-LOS (NLOS) effects are unavoidable in practical situations. Data that considerably deviate from the majority of grouped observations are referred to as outliers (NLOS contaminated observations). When an outlier is present, the performance of a non-robust positioning algorithm can be seriously degraded because the time delay may be significantly bigger than the actual time delay. Therefore, we focus on providing a method to determine the position of the target node accurately against the NLOS noise.

Significant research has been conducted on localization problems in LOS circumstances [1], [2], [3], [4], [5], [6]. Nevertheless, recent studies on location in NLOS contexts are still limited. For instance, 1) mathematical optimization [7], [8], [9], [10], [11], 2) robust statistics [12], [13], [14], [15], [16], [17], [18], 3) LOS and NLOS sensor identification [19], [20], [21], and 4) robust filter [22], [23], [24], [25], [26], [27], [28], [29], [30], [31] have all been studied for location estimation under NLOS conditions. The maximum likelihood estimator (MLE) is known to asymptotically attain efficiency. Although the NLOS noise distribution is accessible, the statistics of NLOS noise are typically time-variant. Therefore, estimating the parameters of the LOS/NLOS mixed model using the MLE may not be pratical. As an outlier-resistant method, the maximal correntropy criterion (MCC)

The associate editor coordinating the review of this manuscript and approving it for publication was Cesar Vargas-Rosales.

has recently drawn significant attention [26], [27], [28]. Under mixed LOS/NLOS circumstances, robust Kalman filters outperform the traditional and unscented Kalman filters [26], [27], [28]. However, the MCC-based technique is known to be unstable and may diverge with the use of a small kernel bandwidth. The ranging problem is proposed in a Bayesian manner [32]. For differential received signal intensity localization, model uncertainties for transmit power and path loss exponent are considered [33]. Additionally, the Euclidean distance matrix is used to locate multiple sources [34]. Further, a robust localization method based on the probability density function (PDF) estimation, where the support for the first peak is used to estimate the LOS distance, is proposed. The central concept of this approach is that the LOS distance measurement from the direct path is always shorter than the NLOS distance measurement from the indirect NLOS path. For this algorithm, the kernel density estimation (KDE) method has been employed and this algorithm outperforms the other state-of-the-art methods [35]. The pedestrian dead reckoning and received signal strength index approaches are fused employing the sensor combination. For this, the weight-based optimization is devised to enhance the accuracy and stability of localization [36]. An indoor localization method using support vector regression using the particle swarm optimization [37]. A deep-learning-based anomaly detector is designed to keep the lifelong stability [38]. Furthermore, the k-nearest neighbor (KNN)-based and orthogonal series (OSERIES)-based algorithms can be used for estimating the PDF. The KDE-based robust localization has the limitation that the LOS distance estimate is just determined as the support for the first peak (mode) of the noise distribution. In general, the mean outperforms the mode in terms of the estimation accuracy. In particular, the mode is not desirable when the sample size is small or when the PDF estimate is highly wiggly. Therefore, the improved method is proposed to overcome the weakness of the mode estimate. The proposed methods find the support for the first peak of the noise PDF and inlier candidates using statistical testing. Subsequently, the mean of these LOS distance candidates is calculated. Specifically, the proposed algorithm has the advantage of using multiple samples to estimate the LOS distance, as opposed to a single sample. Furthermore, the Nadaraya-Watson estimate (conditional mean) is obtained to enhance the accuracy of this LOS distance estimate. Then, the variance for this conditional mean is calculated and then the two-step weighted least squares (WLS) method is employed using this information.

The two-mode Gaussian mixture model (GMM) has been widely used and is essential for localization and tracking; however, it is difficult to model the NLOS error distribution accurately. Consequently, the two-mode GMM may contain modeling errors associated with the NLOS distribution. We use simulation to confirm that the proposed techniques still work for various NLOS models, such as heavy-tailed skew-t [39], [40], [41], [42], Gaussian-uniform mixture [43], [44] and Gaussian-exponential mixture distributions [45]. The proposed robust localization methods do not require any prior information for NLOS errors and only postulate the measurement noise variance is known *a priori*. Also, the proposed robust localization algorithms use TOA observations, but can be employed even when TDOA, RSS or AOA are utilized.

The proposed localization method is a centralized method, but may be implemented with the existing distributed localization method. However, there would be problems such as high energy consumption, increased complexity and error propagation compared to the centralized method. Furthermore, the proposed method may be designed in the cooperative manner [46], [47] to improve localization accuracy and robustness to challenging environments and increase the scalability and coverage. Sensor nodes can exchange information and measurements among the participating entities to improve the accuracy and reliability of individual localization estimates. The critical issue is to develop an individual localization algorithm with improved efficiency and accuracy. In this work, the localization algorithm to improve the accuracy of the individual localization method is studied. In general, the better is the performance of the individual localization method, the better is the performance of the cooperative localization method. In addition, the factor graph method is exploited in the sensor network localization [48]. The NLOS problem may trigger problems such as inaccurate measurements and convergence issue; therefore, the outlier must be effectively discerned and removed therein. Outlier rejection methods or sensor fusion can be applied to identify and discard outlier measurements before they are incorporated into the factor graph. The important point is whether the development of the criterion with which the inlier and outlier are distinguished is possible. The threshold for outlier detection must be set in an optimal manner, which is not an easy task. The generalized likelihood ratio test (GLRT) or Rao-test can be used, but it requires the MLE. The outlier testing should be performed sample by sample to obtain more inlier samples to enhance the localization accuracy. However, the theoretical backgrounds for single observation-based testing are uncommon compared to the asymptotic theory for large sample-based testing.

The key contributions of this study are summarized as follows:

- Using multiple observations and a two-mode GMM, we design the robust KNN-based and OSERIES-based WLS localization algorithms, where the LOS distance is estimated using the KNN- or OSERIES-based PDF estimation method.
- The statistical testing using the Rao criterion to determine the inlier and outlier in the context of LOS/NLOS mixed localization is proven to be the uniformly most powerful (UMP) testing based on the monotone likelihood ratio property [49]. Although this testing has been widely used to discern the inliers and outliers, the proof

that this testing is the UMP testing in the context of the two-mode GMM has not yet been reported to the authors' knowledge.
- The proposed approaches established in the two-mode GMM use the mean that is calculated from measurements obtained from the statistical testing not the mode. The proposed localization methods outperform the conventional method in terms of accuracy because the mean is generally better than the mode [50].
- The conditional variance of the range measurement is shown to be approximately $2\sigma_1^2$, where σ_1^2 is the LOS measurement variance. The conditional variance is then utilized to calculate the weight in the two-step WLS method.

The remainder of this paper is structured as follows. The mixed LOS/NLOS location estimation problem is stated in Section II. Existing techniques are briefly introduced in Section III. The proposed KNN-based and OSERIES-based WLS localization methods are introduced in Section IV. Further, a theoretical examination of the mean square error (MSE) of the proposed estimators is presented in Section V. Based on the results of the simulation, Section VI assesses the root mean square error (RMSE) performance. Experiments conducted using real data and computational complexity analysis are described in Sections VII and VIII, respectively. Finally, conclusions and future works are presented in Section IX.

II. PROBLEM STATEMENT

The goal of the emitter localization approach is to find the solution with which the objective function is minimized. In the case of source location under mixed LOS/NLOS situations, the measurement equation is given as

$$\begin{aligned} r_{i,j} &= d_i + n_{i,j} \\ &= \sqrt{(x-x_i)^2 + (y-y_i)^2} + n_{i,j}, \end{aligned} \tag{1}$$

where $n_{i,j}$ is a two-mode Gaussian mixture random variable defined as $(1-\nu_i)\mathcal{N}(0,\sigma_1^2) + \nu_i\mathcal{N}(\mu_2,\sigma_2^2), i = 1,2,\ldots,M, \quad j = 1,2,\ldots,P$ with M and P denoting the number of sensors and observations in each sensor, respectively. The inliers follow $\mathcal{N}(0,\sigma_1^2)$ and the outliers follow $\mathcal{N}(\mu_2,\sigma_2^2)$, where $\mathcal{N}(\mu_l,\sigma_l^2)$ indicates a Gaussian PDF with mean μ_l and variance σ_l^2 $(l = 1, 2)$. The contamination ratio, which in this case is $\nu_i \in [0, 1]$, is usually lower than 0.5 [12] except for heavily NLOS contaminated situations. The GMM with two modes has been widely used for modeling mixed LOS/NLOS scenarios [17], [18], [19], [20], [21], [22], [23], [24], [25]. Other NLOS error distributions have been identified as the heavy-tailed skew-t, the Gaussian-uniform mixture and the Gaussian-exponential mixture distributions [39], [40], [41], [42], [43], [44], [45]. It may be impossible to acquire the information such as statistical moments of the NLOS noise distribution in practical scenarios. To confirm the robustness against modeling errors through computer simulation, the proposed robust localization algorithms are compared with the state-of-the-art techniques under various NLOS error models. Furthermore, $[x_i \;\; y_i]^T$ symbolizes the known Cartesian coordinates of the i^{th} sensor, whereas $[x\; y]^T$ indicates the unknown target node position. Moreover, $r_{i,j}$ is the range observation from the target node to the i^{th} sensor at the j^{th} time instance and d_i is the actual distance. Squaring both sides of (1) and rearranging the equation results in the following.

$$\begin{aligned} x_i x + y_i y - 0.5R + m_{i,j} &= 0.5({x_i}^2 + {y_i}^2 - r_{i,j}^2), \\ i = 1,2,\ldots,M, \quad j &= 1,2,\ldots,P \end{aligned} \tag{2}$$

where $R = x^2 + y^2$, $m_{i,j} = -d_i n_{i,j} - \frac{1}{2}n_{i,j}^2$. Also, the following expression is obtained by representing (2) in a matrix form

$$Ax + m_j = b_j, \qquad j = 1, \cdots, P \tag{3}$$

where $m_j = [m_{1,j}, \cdots, m_{M,j}]^T$, $x = [x\; y\; R\;]^T$,

$$A = \begin{pmatrix} x_1 & y_1 & -0.5 \\ \vdots & \vdots & \vdots \\ x_M & y_M & -0.5 \end{pmatrix} \tag{4}$$

$$\text{and} \;\; b_j = [b_{1,j} \cdots b_{M,j}]^T = \frac{1}{2}\begin{pmatrix} x_1^2 + y_1^2 - r_{1,j}^2 \\ \vdots \\ x_M^2 + y_M^2 - r_{M,j}^2 \end{pmatrix}. \tag{5}$$

It is expected to estimate the unknown location parameter $\mathbf{x}$ by optimally combining the transformed distance observations, $[b_1, \cdots, b_P]$. Owing to its simplicity, the two-step WLS method has been often utilized. In this study, an uppercase and lowercase boldface letter are used to denote a matrix and vector, respectively. The transpose is represented by the operator $[\cdot]^T$.

III. BACKGROUND

In this section, the Rao detector and UMP testing are introduced. This hypothesis testing approach is used for identification of outliers in the robust localization. In addition, the KNN-based and OSERIES-based PDF estimation methods are presented. These PDF estimation approaches are utilized for finding the support for the first peak (mode) of the distance distribution. There are two approaches of the PDF estimation. The one is the parametric PDF estimation and the other is the non-parametric PDF estimation. The parametric density estimation assumes that the underlying PDF belongs to a specific PDF, such as the Gaussian distribution. This estimation method estimates the parameters of the assumed distribution from the available data. When the underlying distribution is estimated accurately, the parametric PDF estimation can be more efficient than non-parametric PDF estimation. However, the parametric PDF estimation cannot capture the actual distribution in many real-world situations because the assumption of a specific parameter estimation may be too restrictive. In cases where the distribution is complex or multi-modal, finding an appropriate parametric form

can be challenging. On the other hand, the non-parametric PDF estimation makes no assumption about the specific form of the underlying distribution. Instead, it estimates the PDF directly from the data itself, without any prior assumptions. It can handle complex and multi-modal distributions more effectively, as it does not postulate any specific form on the data. Non-parametric methods are generally more robust to outliers or deviations from assumed parametric forms. However, it may require a larger sample size to obtain accurate density estimates than that of parametric methods.

A. THE RAO DETECTOR [51]

In composite hypothesis testing, GLRT has been widely used for discerning the hypotheses [51]. The Rao detector can also be used instead of GLRT. The Rao detector has the advantage that the testing statistic may be easier to compute compared to GLRT and Wald testing and it does not require the determination of the MLE under the alternative hypothesis. The Rao detector decides the alternative hypothesis (H_1) if

$$T_R(r_{i,j}) = I^{-1}(\boldsymbol{\theta} = \boldsymbol{\theta}_0)\left(\frac{\partial \ln p(r_{i,j};\boldsymbol{\theta})}{\partial \boldsymbol{\theta}}\bigg|_{\boldsymbol{\theta}=\boldsymbol{\theta}_0}\right)^2 > \gamma \quad (6)$$

where $H_0 : \boldsymbol{\theta} = \boldsymbol{\theta}_0$, $H_1 : \boldsymbol{\theta} = \boldsymbol{\theta}_1$, $I(\cdot)$ is the Fisher information and γ is the threshold. Otherwise, the Rao detector determines the null hypothesis, H_0.

B. UMP TESTING [49]

Likelihood ratio testing (LRT) is known to be the most powerful testing when all the parameters of the PDFs are accurately known. Namely, LRT is the optimal test under the simple hypothesis. However, the parameters of PDF are difficult to accurately capture in practical scenarios, that is, LRT may not be optimal under the composite hypothesis. Accordingly, optimal testing for the entire set of unknown parameters is required, which is referred to as UMP testing. A test is defined as a UMP test of size (false alarm probability) α if its power (detection probability) is uniformly greater than the power of any other test whose size is less than or equal to α. The Karlin-Rubin theorem can be applied to confirm whether a test is a UMP test, but it cannot be applied when the PDF is parameterized by multiple unknown parameters. In this case, the monotone likelihood ratio (MLR) property can be used to check whether any test is a UMP test (for more details, see [49]). For two-sided tests, the UMP test usually does not exist. In this case, GLRT or maximally invariant tests can be used.

C. KNN-BASED PDF ESTIMATION

The KNN-based PDF estimation method adapts the amount of smoothing according to the local density of observations. The degree of smoothing is controlled using an integer K, typically chosen as $K = \lceil\sqrt{P}\rceil$ [52], where $\lceil x\rceil$ denotes the ceiling function that returns the least integer greater than or equal to x. Then, the KNN-based PDF estimate is defined as follows [52]:

$$\hat{p}(t) = \frac{K}{2Pd_K(t)} \quad (7)$$

where $d_1(t) \le d_2(t) \le \cdots \le d_P(t)$ denote the distances arranged in ascending order, from t to the points of the sample. Generally, the PDF estimate obtained by the KNN method is wigglier than that using the KDE method. Therefore, the first mode of the density estimate may not be consistent with the actual first mode of the PDF. The solution to this problem will be presented in the next section.

D. OSERIES-BASED PDF ESTIMATION

The PDF estimate by OSERIES is calculated as the sum of orthogonal bases, which are multiplied by the weights as follows [53]:

$$\hat{p}(t) = \sum_{l=1}^{\hat{L}} \hat{\beta}_l q_l(t) \quad (8)$$

where $\hat{\beta}_l = \frac{1}{P}\sum_{j=1}^{P} q_l(r_{i,j})$, $q_l(t)$ denotes the l^{th} orthogonal basis, $\hat{L} = \min_L \hat{R}(L)$ for $1 \le L \le s = \lceil\sqrt{P}\rceil$, $\hat{R}(L) = \sum_{l=1}^{L}\frac{\hat{\sigma}_l^2}{P} + \sum_{l=L+1}^{s}(\hat{\beta}_l^2 - \frac{\hat{\sigma}_l^2}{P})_+$, $a_+ = \max(a, 0)$, and $\hat{\sigma}_l^2 = \frac{1}{P-1}\sum_{j=1}^{P}(q_l(r_{i,j}) - \hat{\beta}_l)^2$. $\hat{\beta}_l$ is known to be an unbiased estimator of β_l. Also, L is a smoothing parameter. When L is large, the bias is small and vice versa.

IV. PROPOSED ROBUST LOCALIZATION APPROACHES

In this section, the proposed KNN and OSERIES-based positioning methods are presented. First, the outlier identification testing using the Rao-detection is derived. Furthermore, the robust localization methods based on the KNN and OSERIES-based PDF estimation are presented.

A. DERIVATION OF OUTLIER DETECTION METHOD BASED ON THE RAO TEST

The Rao-test statistic in the robust localization context is derived from definition (6) as follows:

$$T_R(r_{i,j}) = I^{-1}(\mu_2 = 0)\left(\frac{\partial \ln p(r_{i,j};\mu_2)}{\partial \mu_2}\bigg|_{\mu_2=0}\right)^2 \quad (9)$$

$$= \frac{(r_{i,j} - d_i)^2}{\sigma_1^2} \quad (10)$$

where $p(r_{i,j};\mu_2) = \frac{1}{\sqrt{2\pi}\sigma_1}\exp(-\frac{(r_{i,j}-d_i-\mu_2)^2}{2\sigma_1^2})$.

The Rao-test decides that the corresponding sample is an outlier if

$$T_R(r_{i,j}) = \frac{(r_{i,j} - d_i)^2}{\sigma_1^2} > \gamma. \quad (11)$$

That is, the Rao-test decides the LOS state if the null hypothesis (H_0) that the measurement bias (μ_2) is zero is not rejected. On the other hand, the Rao-test decides the NLOS state if the alternative hypothesis (H_1) that the measurement bias is the positive value is accepted. In general, the inlier observation

variance, σ_1^2, is assumed to be known in the localization context and d_i is estimated using the PDF estimation method, which will be presented in Section IV. The testing threshold (γ) is determined by the Neyman-Pearson rule (NP-rule) [51]. That is, $\gamma = Q_{\chi_1^2}^{-1}(P_{FA})$, where $Q^{-1}(\cdot)$ is the inverse Q function, χ_1^2 is the chi-square distribution with one degree-of-freedom and P_{FA} is the false alarm probability. The proposed testing method is proven to be the UMP test in Appendix A.

B. KNN-BASED WLS METHOD

The KNN-based PDF estimation method was introduced in the Section III. The KNN-based WLS method is presented in this section. The LOS distance observation is always smaller than the NLOS distance measurement due to the positive multipath bias. The LOS distance ($\hat{d}_i$) is estimated in advance by capturing the range PDF and searching for the support for the first peak of the PDF of the distance observation. The support for the first peak is determined by finding the smallest support whose frequency (height) is greater than the frequencies of two nearby (adjacent) interpolated grids. However, the PDF estimate by the KNN-based method is significantly wiggly; thus, the support for the first peak may not be enough to be regarded as the accurate inlier estimate. Further, the mean estimate is generally better than the mode estimate with respect to the estimation accuracy [50]. Therefore, we employ the robust testing developed in Section IV. A to identify inlier candidates. Namely, the inlier candidates are selected based on observations satisfying the following:

$$\frac{(r_{i,j} - \hat{d}_i)^2}{\sigma_1^2} < \gamma \tag{12}$$

where the testing threshold (γ) is determined by the NP-rule. Then, the average of these inlier candidates is calculated as

$$\hat{d}_i^m = \frac{\sum_{j \in L} r_{i,j}}{P - Q} \tag{13}$$

where L is the LOS set composed of the LOS samples predicted using the proposed statistical testing, Q is the number of samples that belong to L^c and L^c is the complementary set of L (NLOS set). Furthermore, L and L^c are disjoint sets. This distance estimate is improved using the non-parametric conditional mean, namely the non-parametric regression (Nadaraya-Watson estimator) [52]. That is, the improved distance estimate ($\hat{m}(\hat{d}_i^m)$) is obtained as follows:

$$\hat{m}(\hat{d}_i^m) = \hat{E}[r_i|\hat{d}_i^m] = \frac{\sum_{j=1}^{P} r_{i,j} K(\frac{\hat{d}_i^m - r_{i,j}}{h})}{\sum_{j=1}^{P} K(\frac{\hat{d}_i^m - r_{i,j}}{h})} \tag{14}$$

where $K(u) = \frac{1}{\sqrt{2\pi}} \exp(-\frac{u^2}{2})$ when the Gaussian kernel is employed. Without loss of generality, the kernel bandwidth (h) is set to σ_1^2. Subsequently, $\mathrm{Var}[r_i|\hat{d}_i^m]$ is calculated as follows (the derivation is provided in Appendix B):

$$\mathrm{Var}[r_i|\hat{d}_i^m] \simeq 2\sigma_1^2. \tag{15}$$

In addition, the variance of the estimate for the conditional mean can be calculated as follows [52]:

$$\mathrm{Var}[\hat{m}(\hat{d}_i^m)] = \frac{1}{Ph} \frac{\mathrm{Var}[r_i|\hat{d}_i^m]}{p(\hat{d}_i^m)} \int (K(u))^2 du \tag{16}$$

where $p(\hat{d}_i^m)$ is approximately found using the KDE method and $\int (K(u))^2 du = \frac{1}{2\sqrt{\pi}}$ when the Gaussian kernel is used [52]. The first-step WLS estimate by the KNN-based PDF estimation is calculated as follows:

$$\hat{x} = (A^T C_{\boldsymbol{\mu}_{b,1}}^{-1} A)^{-1} A^T C_{\boldsymbol{\mu}_{b,1}}^{-1} \boldsymbol{\mu}_{b,1} \tag{17}$$

where $\boldsymbol{\mu}_{b,1} = [\mu_{b_1,1}, \cdots, \mu_{b_M,1}]^T$, $\mu_{b_i,1} = \frac{x_i^2 + y_i^2 - (\hat{m}(\hat{d}_i^m))^2}{2}$, $C_{\boldsymbol{\mu}_{b,1}} = (\mathrm{diag}[\sigma^2_{\mu_{b_1,1}}, \cdots, \sigma^2_{\mu_{b_M,1}}])$, $\sigma^2_{\mu_{b_i,1}} \simeq (\hat{m}_i(\hat{d}_i^m))^2 \times \mathrm{Var}(\hat{m}_i(\hat{d}_i^m))$. Further, the second-step estimate can be expressed as follows:

$$\hat{x}_s = (H^T C_{\hat{h}}^{-1} H)^{-1} H^T C_{\hat{h}}^{-1} \hat{h} \tag{18}$$

where the subscript s denotes the second-step estimate,

$$\hat{h} = \left[[\hat{x}]_1^2 \; [\hat{x}]_2^2 \; [\hat{x}]_3 \right]^T, \tag{19}$$

$$H = \begin{pmatrix} 1 & 0 \\ 0 & 1 \\ 1 & 1 \end{pmatrix}, \tag{20}$$

$$\begin{aligned} C_{\hat{h}} &= \mathrm{diag}[2x \; 2y \; 1](A^T C_{\boldsymbol{\mu}_{b,1}}^{-1} A)^{-1} \mathrm{diag}[2x \; 2y \; 1] \\ &\simeq \mathrm{diag}[2[\hat{x}]_1 \; 2[\hat{x}]_2 \; 1](A^T C_{\boldsymbol{\mu}_{b,1}}^{-1} A)^{-1} \mathrm{diag}[2[\hat{x}]_1 \; 2[\hat{x}]_2 \; 1], \end{aligned} \tag{21}$$

and $[\hat{x}]_i$ ($i = 1,2,3$) is the i^{th} component of $\hat{x}$. The final emitter position estimate can be expressed as follows:

$$\hat{x}_f = \left[\mathrm{sgn}([\hat{x}]_1)\sqrt{[\hat{x}_s]_1} \;\; \mathrm{sgn}([\hat{x}]_2)\sqrt{[\hat{x}_s]_2} \right]^T \tag{22}$$

where $\mathrm{sgn}(\cdot)$ indicates the sign function and $[\hat{x}_s]_i$ ($i = 1,2$) is the i^{th} component of the second-step position estimate.

Remark: The variance of $\hat{m}(\hat{d}_i^m)$ can also be calculated from (14) by considering the $K(\cdot)$ as a fixed value. It has the advantage that the $\mathrm{Var}[r_i|\hat{d}_i^m]$ is not required, but the RMSE performance using (14) was slightly degraded compared to the method using (16) in the performance testing.

C. OSERIES-BASED WLS METHOD

The OSERIES-based PDF estimation method was presented in Section III. The robust localization algorithm based on the OSERIES-based PDF estimator is investigated in this section. The OSERIES-based robust localization differs from the KNN-based positioning method in that it uses the orthogonal basis to estimate the PDF of distance measurements. In this study, the cosine basis is used, defined as $\phi_0(x) = 1$ and $\phi_j(x) = \sqrt{2}\cos(j\pi x)$ for $j \geq 1$. The remainders are the same as the robust localization method using the KNN-based PDF estimation algorithm. Moreover, the PDF estimate may have a negative value, but this property is not a problem for determining the peaks of the PDF estimate.

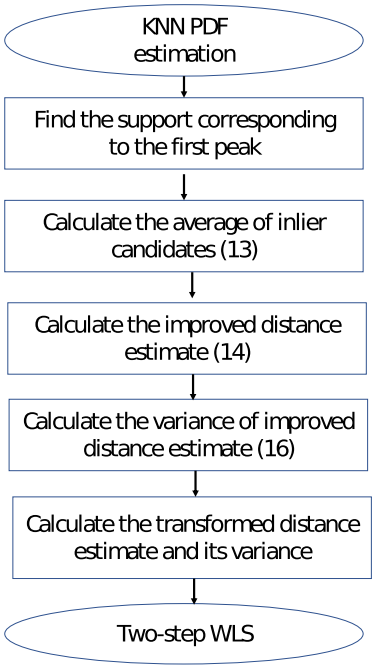

FIGURE 1. Flow chart of the KNN PDF estimation-based WLS algorithm.

We summarize the KNN and OSERIES-based WLS algorithms in Algorithm 1 and 2, respectively. In addition, the flowchart of the KNN-based WLS method is given in Fig. 1.

Algorithm 1 KNN-Based WLS Algorithm

Step 1. KNN PDF estimation is performed.
Step 2. Find the support corresponding to the first peak of the PDF that is estimated by KNN method ($\hat{d}_i$).
Step 3. $\hat{d}_i^m$ is calculated using (13).
Step 4. $\hat{m}(\hat{d}_i^m)$ is calculated using (14).
Step 5. $\mathrm{Var}[r_i|\hat{d}_i^m]$ is obtained using (15).
Step 6. $\mathrm{Var}[\hat{m}(\hat{d}_i^m)]$ is calculated using (16).
Step 7. The transformed distance estimate is calculated: $\hat{b}_i = \frac{x_i^2+y_i^2-(\hat{m}(\hat{d}_i^m))^2}{2}$.
Step 8. The variance of the transformed distance estimate is calculated as: $\mathrm{Var}[\hat{b}_i] \simeq (\hat{m}(\hat{d}_i^m))^2\mathrm{Var}[\hat{m}(\hat{d}_i^m)]$.
Step 9. Determine the source coordinates using the two-step WLS method.

Algorithm 2 OSERIES-Based WLS Algorithm

Step 1. Orthogonal series PDF estimation is performed.
Step 2. Find the support corresponding to the first peak of the PDF that is estimated by OSERIES-based method ($\hat{d}_i$).
Step 3−**Step 9**. Identical with that of Algorithm 1.

V. MSE PERFORMANCE ANALYSIS

In this section, the MSE performance of the proposed robust algorithms is analyzed. First, the estimation bias is derived as follows:

$$\mathrm{Bias}[\hat{x}_f] = [E\{\mathrm{sgn}([\hat{x}]_1)\sqrt{[\hat{x}_s]_1} - x\}\ E\{\mathrm{sgn}([\hat{x}]_2)\sqrt{[\hat{x}_s]_2} - y\}]^T \tag{23}$$

$$\simeq [\mathrm{sgn}(x)E\{(\sqrt{[\hat{x}_s]_1} - |x|)\}\ \mathrm{sgn}(y)E\{(\sqrt{[\hat{x}_s]_2} - |y|)\}]^T \tag{24}$$

$$\simeq \left[\mathrm{sgn}(x)E\left\{\frac{([\hat{x}_s]_1 - x^2)}{2|x|}\right\}\ \mathrm{sgn}(y)E\left\{\frac{([\hat{x}_s]_2 - y^2)}{2|y|}\right\}\right]^T \tag{25}$$

$$= \left[\frac{1}{2x}E\{([\hat{x}_s]_1 - x^2)\}\ \frac{1}{2y}E\{([\hat{x}_s]_2 - y^2)\}\right]^T \tag{26}$$

$$= D_2^{-1}(H^T C_{\widehat{h}}^{-1}H)^{-1}H^T C_{\widehat{h}}^{-1}(E[\widehat{h}] - Hx_s) \tag{27}$$

$$\simeq D_2^{-1}(H^T C_{\widehat{h}}^{-1}H)^{-1}H^T C_{\widehat{h}}^{-1}D_1(E[\widehat{x}] - x) \tag{28}$$

$$= D_2^{-1}(H^T C_{\widehat{h}}^{-1}H)^{-1}H^T C_{\widehat{h}}^{-1}D_1 \times (A^T C_{\boldsymbol{\mu}_{b,1}}^{-1}A)^{-1}\mathbf{A}^T C_{\boldsymbol{\mu}_{b,1}}^{-1}(E[\boldsymbol{\mu}_{b,1}] - Ax) \tag{29}$$

where $x_s = [x^2\ \ y^2]^T$, $D_1 = \mathrm{diag}[2x\ \ 2y\ \ 1]$ and $D_2 = \mathrm{diag}[2x\ \ 2y]$. In the derivation of (24), the high signal-to-noise ratio (SNR) condition is assumed. Furthermore, the Taylor-series approximation is utilized in the derivation of (25). Generally, $E[\boldsymbol{\mu}_{b,1}]$ is difficult to calculate. Therefore, the estimation bias is obtained by the Monte-Carlo approach (for more details, refer to [15]). Next, the estimation error variance is derived as follows (for more details, refer to [15]):

$$\mathrm{Cov}[\Delta\hat{x}_f] = G(A^T C_{\boldsymbol{\mu}_{b,1}}^{-1}A)^{-1}G^T \tag{30}$$

where $G = D_2^{-1}(H^T C_{\widehat{h}}^{-1}H)^{-1}H^T C_{\widehat{h}}^{-1}D_1$. Finally, the MSE is obtained as follows:

$$\mathrm{MSE}(\hat{x}_f) = \mathrm{tr}(\mathrm{Cov}[\Delta\hat{x}_f]) + ||\mathrm{Bias}(\hat{x}_f)||_2^2 \tag{31}$$

where $\mathrm{tr}(\cdot)$ is the abbreviation of trace operator and $||\cdot||_2$ denotes the 2-norm.

VI. SIMULATION RESULTS

In this section, the accuracies of the KNN and OSERIES-based WLS methods were compared with that of the adaptive MCC (AMCC) EKF [27], statistical similarity measure (SSM)-based Kalman filter [31], KDE-based WLS algorithm [35] and skipped filter WLS method [54] in this section.

A. SIMULATION PARAMETERS

The localization accuracy is evaluated in relation to RMSE and is defined as (33):

$$\mathrm{RMSE} = \sqrt{\frac{\sum_{i=1}^{10}\sum_{k=1}^{300}[(\hat{x}^k(i) - x(i))^2 + (\hat{y}^k(i) - y(i))^2]}{10 \times 300}} \tag{32}$$

where $[\hat{x}^k(i),\ \ \hat{y}^k(i)]^T$ is Cartesian coordinates of the point target node in the i^{th} position set and k^{th} iteration. Additionally, $x(i)$ and $y(i)$ indicate the real position coordinates of the emitter at the i^{th} position. The placement of the sources and

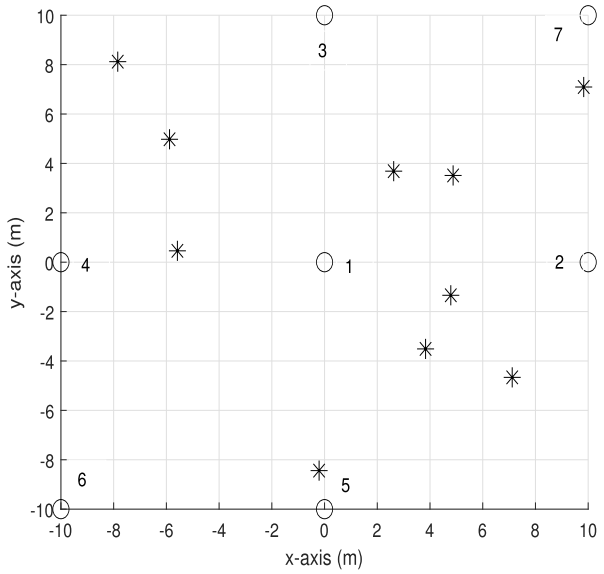

FIGURE 2. Sensor and source deployment, with white circles for sensors and asterisks for sources.

sensors is shown in Fig. 2 as circles and asterisks, respectively. The sensor deployment of Fig. 2 is chosen because it makes the geometric dilution of precision be low (the larger the area formed by the sensors and source, the better (lower) the value of the GDOP and vice versa). In addition, the proposed algorithms can be used for the other sensor network deployment unless the deployment shape is the specific form such as a linear array.

B. GENERAL RESULTS

Figure 3 shows the localization accuracy for various standard deviations of the NLOS error. Sensors 4, 5, 6 and 7 were LOS/NLOS mixture sensors as shown in Fig. 3(a) and the standard deviation (σ_1) of LOS noise was 0.6 m. The measurement bias (μ_2) was set at 5 m. The standard deviation of LOS measurement noise was set to a lower value than that of NLOS noise (σ_2). The RMSE of the KNN WLS technique and the OSERIES-based WLS method was the lowest among robust localization approaches, as illustrated in Figs. 3(a)-(c). Additionally, the NLOS noise had little impact on the RMSE of any approach.

The RMSEs with regard to the LOS noise standard deviation for various mixture LOS/NLOS sensor numbers are shown in Fig. 4. Sensors 5, 6 and 7 were considered as LOS/NLOS mixture sensors, as indicated in Fig. 4(a). The remaining sensors were LOS/NLOS mixture sensors. Further, sensors 4, 5, 6 and 7 were LOS/NLOS mixture sensors in Fig. 4(b), and sensors 3, 4, 5, 6 and 7 were LOS/NLOS mixture sensors in Fig. 4(c). As the LOS noise standard deviation increased, so did the RMSEs of all localization techniques, as shown in Figs. 4(a)-(c). In low-noise settings, the RMSEs of the proposed KNN WLS and OSERIES WLS methods were close to the CRLB and outperformed the other existing approaches as the noise level increased. In particular,

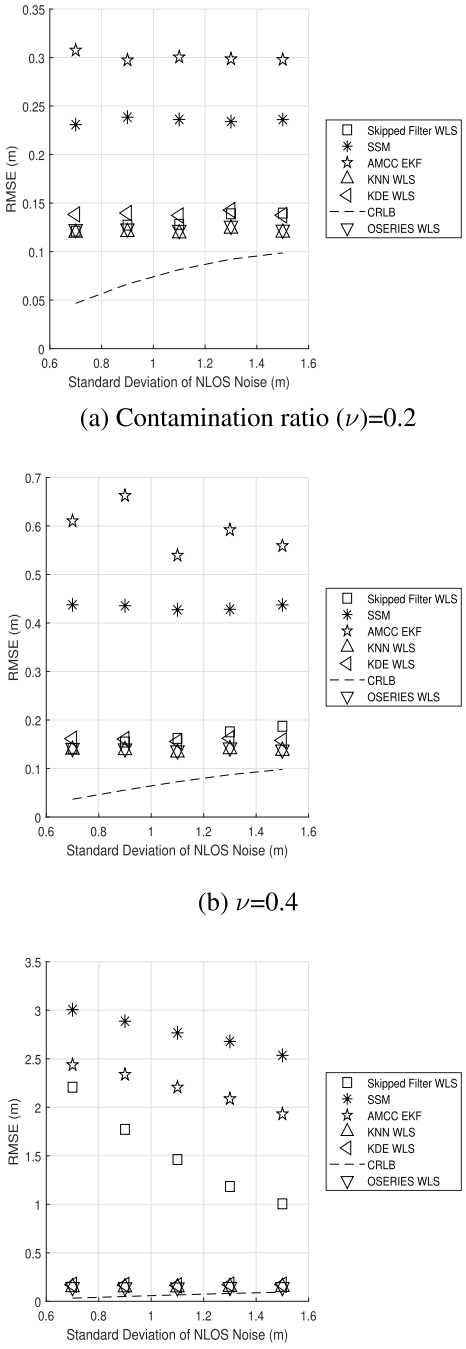

(a) Contamination ratio (ν)=0.2

(b) ν=0.4

(c) ν=0.6

FIGURE 3. RMSEs of the robust localization algorithms for various contamination ratios (ν) and various NLOS noise standard deviation values when sensors 4, 5, 6 and 7 are LOS/NLOS mixture sensors (σ_1: 0.6 m, μ_2: 5 m).

the OSERIES WLS method was slightly superior to the KNN WLS method in large noise conditions. It should be noted that although more than half of sensors are contaminated by the NLOS noise, the robust localization performance was maintained when the contamination ratio was less than 0.5. This is the advantage of the multiple sample-based algorithm compared to the one sample-based method.

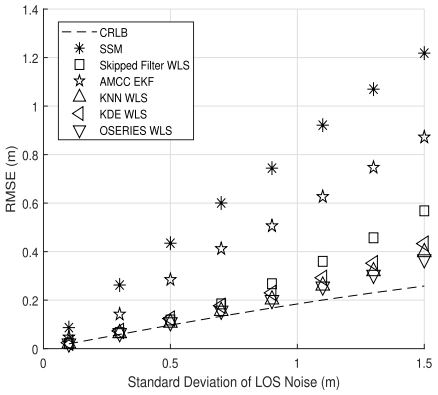

(a) Standard deviation of NLOS noise (σ_2): 4 m, measurement bias (μ_2): 5 m, ν=0.4, sensors 5, 6 and 7 are LOS/NLOS mixture sensors.

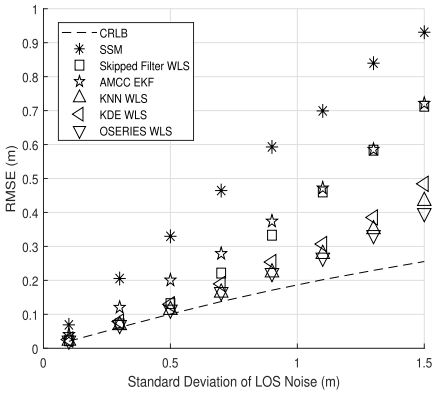

(b) σ_2: 4 m, μ_2: 5 m, ν=0.4, sensors 4, 5, 6 and 7 are LOS/NLOS mixture sensors.

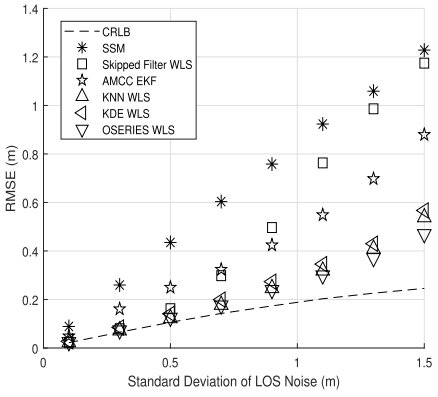

(c) σ_2: 4 m, μ_2: 5 m, ν=0.4, sensors 3, 4, 5, 6 and 7 are LOS/NLOS mixture sensors.

FIGURE 4. RMSEs of the robust localization techniques for various LOS noise standard deviations for varying LOS/NLOS mixture sensor numbers.

Sensors 4-7 were taken for LOS/NLOS mixture sensors in Figs. 5-8. The RMSEs with respect to the measurement bias (μ_2) were shown in Fig. 5. The RMSEs of the KNN WLS and OSERIES WLS methods were not significantly

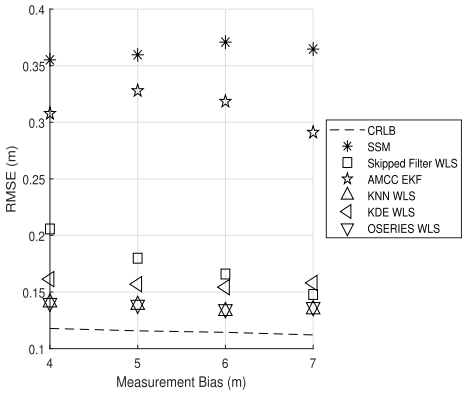

FIGURE 5. RMSEs of the robust location algorithms at various measurement bias (σ_2: 4 m, σ_1: 0.6 m, $\nu = 0.4$).

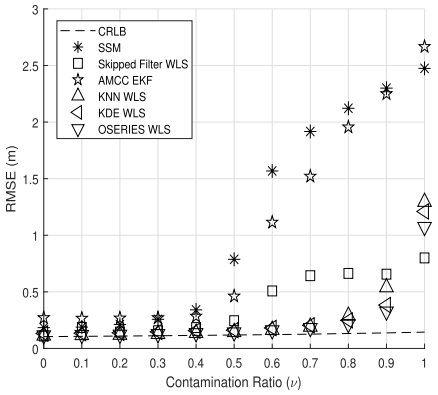

FIGURE 6. RMSEs of the robust positioning techniques at various contamination ratio (ν) (σ_2: 4 m, σ_1: 0.6 m).

impacted by the measurement bias, as shown in Fig. 5. The RMSEs of the proposed KNN WLS and OSERIES WLS methods were lower than those of the other methods and just slightly higher than the CRLB. In general, the RMSE decreases when the measurement bias increases because the LOS and NLOS samples can be more accurately discerned in the outlier identification step.

The RMSEs were depicted in Fig. 6 as a function of the contamination ratio. For a low contamination ratio (below 0.5), the RMSEs of the KNN WLS and OSERIES WLS techniques were comparable, but the RMSE of the OSERIES WLS method was the lowest among the localization algorithms for a high contamination ratio. Meanwhile, as the contamination ratio exceeded 0.5, the RMSEs of the SSM, AMCC EKF and skipped filter WLS techniques increased gradually or significantly.

The RMSEs were shown as a function of sample size in Fig. 7. The accuracies of the KNN WLS and OSERIES WLS methods were greater than those of the other methods, as shown in Fig. 7 and all the robust approaches performed better. The RMSEs of the KNN WLS and OSERIES WLS methods were closer to the CRLB with an increase in the sample size. When the sample size increases, the variance of the estimated PDF decreases and the estimate becomes more

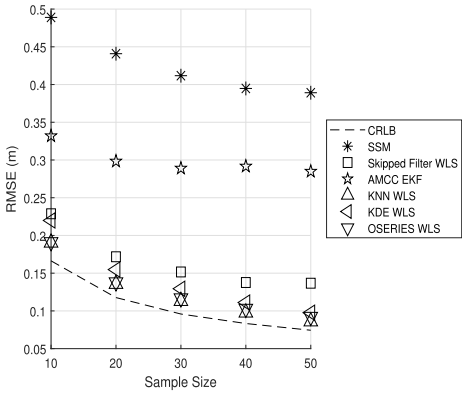

FIGURE 7. RMSEs of the robust localization approaches at various sample size (σ_2: 4 m, σ_1: 0.6 m, $\nu = 0.4$).

stable and less sensitive to individual data points or random variations in the data. This leads to a more reliable estimation of the underlying PDF.

The robustness of the proposed approaches against the NLOS noise modeling error was then tested. Accurately capturing the NLOS error distribution is challenging, even though the proposed methods were developed in the formulation of the two-mode GMM in this study. As a result, a modeling error may exist. Various noise models, such as the skew-t distribution [39], [40], [41], [42], Gaussian-uniform mixture distribution [43], [44] and Gaussian-exponential mixture distribution [45], are available. To determine whether the KNN and OSERIES-based WLS algorithms remain effective under the various NLOS error distributions, we performed a simulation. When the NLOS error follows the skew-t distribution (degree-of-freedom: 3, skewness: 2), the Gaussian-uniform mixture distribution, where random bias follows the uniform distribution $\mathcal{U}$[0 m, 5 m], and the Gaussian-exponential mixture distribution whose rate parameter is set to $\frac{1}{4}$, simulation results were shown in Figs. 8(a)-(c). The proposed KNN and OSERIES-based WLS approaches still showed lower RMSEs than the conventional methods even for cases except for the two-mode Gaussian mixture distribution. Again, in the large noise settings, the RMSE performances of the KNN WLS and OSERIES WLS techniques were the best and the accuracy of the OSERIES-based WLS method was slightly better than that of the KNN-based WLS method.

In Fig. 9, the RMSEs of the localization algorithms were compared for the sources located with the uniform interval using the Gaussian mixture distribution. The arrangement of sources and sensors was depicted in Fig. 9(a). Further, Fig. 9(b) illustrates the RMSE with respect to the x-axis. The standard deviation of the LOS noise was 1 m, the contamination ratio was 0.4 and the standard deviation of NLOS error was 2 m. Clearly, the RMSE of the proposed OSERIES WLS method was lower than that of the existing methods for all x coordinates. The RMSE was lower near the origin and increased when the source was more distant from the origin. The reason for the increase in the RMSE when distance between the sensor and the object increases is that there is often an increase in the area of the region of ambiguity with

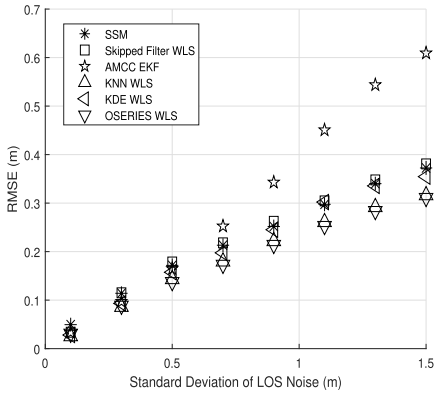

(a) NLOS error: skew-t distribution, degree-of-freedom=3, skewness=2.

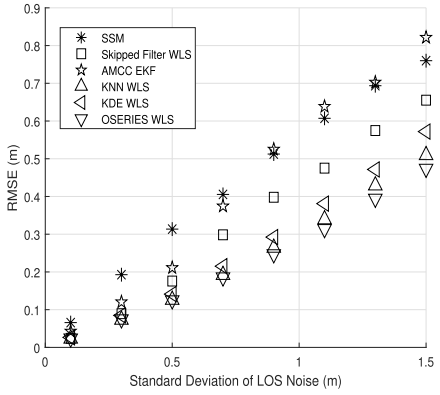

(b) ν=0.4, NLOS measurement bias: $\mathcal{U}$[0 m, 5 m].

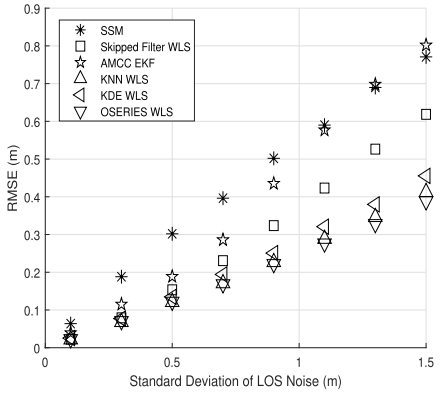

(c) ν=0.4, NLOS measurement bias: Exp($\frac{1}{4}$).

FIGURE 8. RMSEs of the resilient localization techniques at various LOS noise standard deviation values (a) skew-t and (b) Gaussian-uniform mixture (c) Gaussian-exponential mixture distributions.

measurements when the emitter becomes distant from sensor. It was almost symmetric with respect to the origin excluding AMCC EKF.

VII. EXPERIMENT USING THE REAL DATA

In this section, the experimental results using the real data are presented. The real data used in [55] were employed. For details, refer to [55]. Eight sensors were used and their

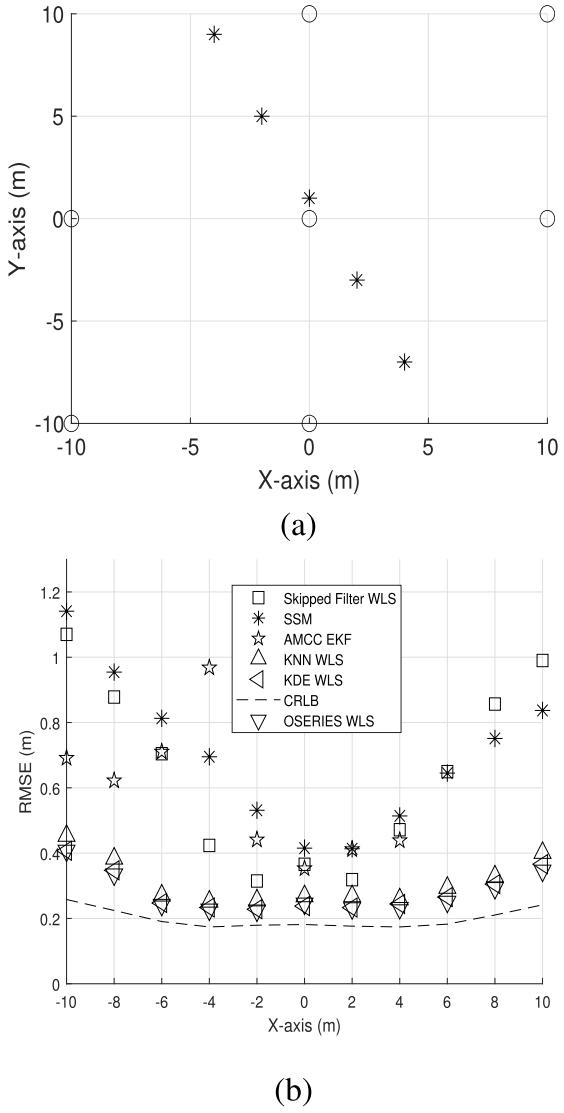

FIGURE 9. Comparison of the RMSEs of localization methods when the emitters are located in the uniform interval under the Gaussian mixture distribution (a) Deployment of tested sources and sensors (b) RMSE versus x-axis coordinates.

positions were [8.47, 11.87, 0.93] m, [8.41, 7.85, 0.69] m, [5.95, 7.45, 0.64] m, [5.45, 6.71, 1.3] m, [6.95, 0.05, 1.43] m, [2.24, 0.05, 1.47] m, [3.06, 8.33, 1.42] m, [4.47, 11.21, 1.42] m. Further, the source location was [1.55, 3.49, 1.2] m. Unlike the simulation part, the three-dimensional localization was performed. Sensors 1, 2, 3 and 4 were NLOS sensors and the others were LOS sensors and ultra-wideband sensors were used. As seen from Table 1, the localization performances of the proposed algorithms were superior to those of other algorithms. Meanwhile, the closed-form skipped filter WLS algorithm showed moderate localization performance. On the other hand, the performance of the robust Kalman filter-based methods was inferior to those of other methods. Apparently, Kalman filter-based algorithms are vulnerable to the multi-modal distribution. The difference between the simulation

TABLE 1. RMSE using real data.

Method	RMSE (m)
SSM	1.3341
Skipped Filter WLS	0.8164
AMCC EKF	1.1294
KNN WLS	0.2273
KDE WLS	0.4214
OSERIES WLS	0.2277

was that the density estimation-based WLS methods used the optimal bandwidth by trial and error to obtain the best performance.

VIII. COMPUTATIONAL COMPLEXITY ANALYSIS

The computational complexity of the Kalman filter-based localization methods was dominated by the covariance update with the complexity of $\mathcal{O}(Md^3)$, where M and d denote the number of sensors and variables in the state, respectively. Furthermore, the computational complexity of the correntropy computation in the AMCC EKF was $\mathcal{O}(MP^2)$, where P is the size of the sample set. Meanwhile, the computational complexity of the density estimation-based WLS localization was $\mathcal{O}(MP^2+MG+d^3)$, where G denotes the number of grids. The computational complexity of the PDF estimation-based WLS methods was higher than that of Kalman filter-based methods because the number of grids is large (set to 1000 in the proposed methods). However, when the number of grids was not large, the computational complexity of the PDF estimation-based WLS methods was similar to that of the Kalman filter-based methods. The computational complexity of the skipped filter WLS method mainly depended on the matrix inversion, whose complexity was $\mathcal{O}(d^3)$. Further, the computational complexity of the skipped filter WLS method was the lowest among the robust localization methods, although it exhibited moderate localization performance.

Discussion: Indeed, the proposed PDF estimation-based localization methods can be used in the static object localization or slow-moving object localization, but may not be appropriate for dynamic object localization because its computational complexity is relatively high and multiple samples-based method.

IX. CONCLUSION

In this study, the two-mode GMM was used to develop the KNN and OSERIES-based WLS approaches. The support for the first peak (mode) of the PDF estimate was determined and then candidates for the LOS distance were identified using the proposed statistical testing. Subsequently, the mean for these samples was calculated and this mean estimate was better than the mode estimate with respect to the estimation accuracy. In addition, the conditional mean (Nadaraya-Watson estimate) was employed to improve the accuracy of the LOS distance estimate. After determining the variance for this distance estimate, the two-step WLS method was used.

Indeed, the proposed localization techniques were resistant to noise model mismatch in simulation results. Moreover, the Rao testing in the context of the two-mode GMM was shown to be the UMP test. Furthermore, the conditional variance of the range observation was derived. The simulation results demonstrated that, under a variety of conditions, the RMSEs of the proposed approaches were superior to the state-of-the-art robust localization methods. Future research would concentrate on developing robust localization algorithms using a single observation.

APPENDIX A
PROOF OF (12) TO BE THE UMP TEST

The likelihood ratio in the two-mode Gaussian distribution case is obtained as follows:

$$L = \frac{\frac{1}{\sqrt{2\pi}\sigma_2}\exp(-\frac{1}{2\sigma_2^2}(r_{i,j}-d_i-\mu_2)^2)}{\frac{1}{\sqrt{2\pi}\sigma_1}\exp(-\frac{1}{2\sigma_1^2}(r_{i,j}-d_i)^2)} \tag{33}$$

$$= \frac{\frac{1}{\sqrt{2\pi}\sigma_2}\exp(-\frac{1}{2\sigma_1^2}\frac{\sigma_1^2}{\sigma_2^2}(r_{i,j}-d_i-\mu_2)^2)}{\frac{1}{\sqrt{2\pi}\sigma_1}\exp(-\frac{1}{2\sigma_1^2}(r_{i,j}-d_i)^2)} \tag{34}$$

Then, the log-likelihood ratio is calculated as follows:

$$l = \ln L$$

$$= \frac{1}{2}\ln\frac{\sigma_1^2}{\sigma_2^2} - \frac{\sigma_1^2}{2\sigma_2^2}\left(\frac{1}{\sigma_1^2}(r_{i,j}-d_i-\mu_2)^2\right) + \frac{1}{2\sigma_1^2}(r_{i,j}-d_i)^2 \tag{35}$$

$$= \frac{1}{2}\ln\frac{\sigma_1^2}{\sigma_2^2} - \frac{\sigma_1^2}{2\sigma_2^2}\left(\frac{1}{\sigma_1^2}((r_{i,j}-d_i)^2+\mu_2^2-2(r_{i,j}-d_i)\mu_2)\right) + \frac{1}{2\sigma_1^2}(r_{i,j}-d_i)^2 \tag{36}$$

$$= \frac{1}{2}\ln\frac{\sigma_1^2}{\sigma_2^2} - \frac{\sigma_1^2}{2\sigma_2^2}\left(T(r_{i,j}) + \frac{\mu_2^2}{\sigma_1^2} - \frac{2}{\sigma_1^2}(r_{i,j}-d_i)\mu_2\right) + \frac{1}{2}T(r_{i,j}) \tag{37}$$

$$= \frac{1}{2}\ln\frac{\sigma_1^2}{\sigma_2^2} + \frac{1}{2}T(r_{i,j}) - \frac{\sigma_1^2}{2\sigma_2^2}\left(T(r_{i,j}) + \frac{\mu_2^2}{\sigma_1^2} - \frac{2\mu_2}{\sigma_1^2}\mathrm{sgn}(r_{i,j}-d_i)|r_{i,j}-d_i|\right) \tag{38}$$

$$= \frac{1}{2}\ln\frac{\sigma_1^2}{\sigma_2^2} + \frac{1}{2}T(r_{i,j}) - \frac{\sigma_1^2}{2\sigma_2^2}\left(T(r_{i,j}) + \frac{\mu_2^2}{\sigma_1^2} - \frac{2\mu_2}{\sigma_1}\mathrm{sgn}(r_{i,j}-d_i)\sqrt{T(r_{i,j})}\right) \tag{39}$$

where $T(r_{i,j}) = \frac{(r_{i,j}-d_i)^2}{\sigma_1^2}$. Furthermore, $\frac{\partial l}{\partial T(r_{i,j})}$ can be divided into two cases, namely, $(r_{i,j}-d_i)$ is positive or negative. If $r_{i,j}-d_i > 0$, $\frac{\partial l}{\partial T(r_{i,j})}$ is calculated as follows:

$$\frac{\partial l}{\partial T(r_{i,j})} = -\frac{\sigma_1^2}{2\sigma_2^2} + \frac{\mu_2\sigma_1}{2\sigma_2^2}\frac{1}{\sqrt{T(r_{i,j})}} + \frac{1}{2} \tag{40}$$

Eq.(40) is always bigger than zero because $\sigma_2^2 > \sigma_1^2$ and $\mu_2 > 0$ when the corresponding observation is the NLOS sample. On the other hand, when $r_{i,j}-d_i < 0$, $\frac{\partial l}{\partial T(r_{i,j})}$ is calculated as follows:

$$\frac{\partial l}{\partial T(r_{i,j})} = -\frac{\sigma_1^2}{2\sigma_2^2} - \frac{\mu_2\sigma_1}{2\sigma_2^2}\frac{1}{\sqrt{T(r_{i,j})}} + \frac{1}{2}. \tag{41}$$

The case that $r_{i,j}-d_i < 0$ is feasible only in the LOS state. Thus, $\frac{\partial l}{\partial T(r_{i,j})}$ is always bigger than zero because $\mu_2 = 0$ and $\sigma_2^2 > \sigma_1^2$. Subsequently, the following threshold test is the UMP test by the MLR property [49]:

$$T(r_{i,j}) \underset{H_0}{\overset{H_1}{\gtrless}} \gamma \tag{42}$$

where γ is determined by the NP-rule.

APPENDIX B
DERIVATION OF Var$[r_i|\hat{d}_i^m]$

The Var$[r_i|\hat{d}_i^m]$ has been derived in [35] as follows:

$$\mathrm{Var}[r_i|\hat{d}_i^m] = \frac{\sum_{j=1}^P K_h(\hat{d}_i^m - r_{i,j})(r_{i,j}-\hat{m}(\hat{d}_i^m))^2}{\sum_{j=1}^P K_h(\hat{d}_i^m - r_{i,j})} + h^2 \tag{43}$$

$$= \frac{\sum_{j=1}^P \exp(-\frac{(\hat{d}_i^m - r_{i,j})^2}{2h^2})(r_{i,j}-\hat{m}(\hat{d}_i^m))^2}{\sum_{j=1}^P \exp(-\frac{(\hat{d}_i^m - r_{i,j})^2}{2h^2})} + h^2. \tag{44}$$

Then, we can further simplify (44) as follows. If the observation $r_{i,j}$ is the inlier, $\exp\left(-\frac{(\hat{d}_i^m - r_{i,j})^2}{2h^2}\right) \simeq 1$ because $(\hat{d}_i^m - r_{i,j})^2$ would be small. On the contrary, if $r_{i,j}$ is the outlier, $\exp\left(-\frac{(\hat{d}_i^m - r_{i,j})^2}{2h^2}\right) \simeq 0$ because $(\hat{d}_i^m - r_{i,j})^2$ would be large. Hence, $\mathrm{Var}[r_i|\hat{d}_i^m] \simeq \frac{\sum_{j\in\mathrm{LOS}}(r_{i,j}-\hat{m}(\hat{d}_i^m))^2}{P-Q} + h^2 \simeq \sigma_1^2 + \sigma_1^2 = 2\sigma_1^2$. Also, $j \in$ LOS indicates the index which belongs to the LOS measurement.

With respect to more rigorous mathematical sense, (44) can be simplified as follows. The approximation that $\hat{d}_i^m \simeq \hat{m}(\hat{d}_i^m)$ is used in (44). Then, Var$[r_i|\hat{d}_i^m]$ can be derived as follows:

$$\mathrm{Var}[r_i|\hat{d}_i^m] = \frac{\sum_{j=1}^P \exp(-\frac{(\hat{d}_i^m - r_{i,j})^2}{2h^2})(r_{i,j}-\hat{m}(\hat{d}_i^m))^2}{\sum_{j=1}^P \exp(-\frac{(\hat{d}_i^m - r_{i,j})^2}{2h^2})} + h^2 \tag{45}$$

$$\simeq \frac{\sum_{j=1}^P \exp(-\frac{(\hat{m}(\hat{d}_i^m) - r_{i,j})^2}{2h^2})(r_{i,j}-\hat{m}(\hat{d}_i^m))^2}{\sum_{j=1}^P \exp(-\frac{(\hat{m}(\hat{d}_i^m) - r_{i,j})^2}{2h^2})} + h^2 \tag{46}$$

$$\simeq \frac{\frac{1}{\sqrt{2\pi}h}\int_{-\infty}^{\infty}\exp(-\frac{(\hat{m}(\hat{d}_i^m) - r_{i,j})^2}{2h^2})(r_{i,j}-\hat{m}(\hat{d}_i^m))^2 dr_{i,j}}{\frac{1}{\sqrt{2\pi}h}\int_{-\infty}^{\infty}\exp(-\frac{(\hat{m}(\hat{d}_i^m) - r_{i,j})^2}{2h^2})dr_{i,j}} + h^2 \tag{47}$$

$$= \frac{\frac{1}{\sqrt{2\pi}} \int_{-\infty}^{\infty} \exp(-\frac{t^2}{2})(ht)^2 dt}{\frac{1}{\sqrt{2\pi}} \int_{-\infty}^{\infty} \exp(-\frac{t^2}{2}) dt} + h^2 \tag{48}$$

$$= h^2 E[t^2] + h^2 \tag{49}$$

$$= h^2 \mathrm{Var}(t) + h^2 \tag{50}$$

$$= h^2 + h^2 \tag{51}$$

$$= 2\sigma_1^2. \tag{52}$$

In the derivation of (47) and (48), the summation is replaced by the integral, $\frac{\hat{m}(\hat{d}_i^m) - r_{i,j}}{h} \triangleq t$ and $\frac{-dr_{i,j}}{h} \triangleq dt$, respectively.

REFERENCES

[1] D. Torrieri, "Statistical theory of passive location systems," *IEEE Trans. Aerosp. Electron. Syst.*, vol. AES-20, no. 2, pp. 183–198, Mar. 1984.

[2] Y. T. Chan and K. C. Ho, "A simple and efficient estimator for hyperbolic location," *IEEE Trans. Signal Process.*, vol. 42, no. 8, pp. 1905–1915, May 1994.

[3] H. C. So and L. Lin, "Linear least squares approach for accurate received signal strength based source localization," *IEEE Trans. Signal Process.*, vol. 59, no. 8, pp. 4035–4040, Aug. 2011.

[4] C. Park and J. Chang, "Closed-form localization for distributed MIMO radar systems using time delay measurements," *IEEE Trans. Wireless Commun.*, vol. 15, no. 2, pp. 1480–1490, Feb. 2016.

[5] C.-H. Park and J.-H. Chang, "Shrinkage estimation-based source localization with minimum mean squared error criterion and minimum bias criterion," *Digit. Signal Process.*, vol. 29, pp. 100–106, Jun. 2014.

[6] J. A. Belloch, A. Gonzalez, A. M. Vidal, and M. Cobos, "On the performance of multi-GPU-based expert systems for acoustic localization involving massive microphone arrays," *Expert Syst. Appl.*, vol. 42, no. 13, pp. 5607–5620, Aug. 2015.

[7] S. Zhang, S. Gao, G. Wang, and Y. Li, "Robust NLOS error mitigation method for TOA-based localization via second-order cone relaxation," *IEEE Commun. Lett.*, vol. 19, no. 12, pp. 2210–2213, Dec. 2015.

[8] G. Wang, H. Chen, Y. Li, and N. Ansari, "NLOS error mitigation for TOA-based localization via convex relaxation," *IEEE Trans. Wireless Commun.*, vol. 13, no. 8, pp. 4119–4131, Aug. 2014.

[9] R. M. Vaghefi, J. Schloemann, and R. M. Buehrer, "NLOS mitigation in TOA-based localization using semidefinite programming," in *Proc. 10th Workshop Positioning, Navigat. Commun. (WPNC)*, Mar. 2013, pp. 1–6.

[10] R. M. Vaghefi and R. M. Buehrer, "Cooperative localization in NLOS environments using semidefinite programming," *IEEE Commun. Lett.*, vol. 19, no. 8, pp. 1382–1385, Aug. 2015.

[11] S. Tomic and M. Beko, "A bisection-based approach for exact target localization in NLOS environments," *Signal Process.*, vol. 143, pp. 328–335, Feb. 2018.

[12] P. J. Rousseeuw and A. M. Leroy, *Robust Regression and Outlier Detection*. Hoboken, NJ, USA: Wiley, 1987.

[13] Z. Li, W. Trappe, Y. Zhang, and B. Nath, "Robust statistical methods for securing wireless localization in sensor networks," in *Proc. 4th Int. Symp. Inf. Process. Sensor Netw.*, Los Angeles, CA, USA, 2005, pp. 91–98.

[14] R. Casas, A. Marco, J. J. Guerrero, and J. Falcó, "Robust estimator for non-line-of-sight error mitigation in indoor localization," *EURASIP J. Adv. Signal Process.*, vol. 2006, no. 1, pp. 1–8, Dec. 2006.

[15] C. Park and J. Chang, "Revisiting skipped filter and development of robust localization method based on variational Bayesian Gaussian mixture algorithm," *IEEE Trans. Signal Process.*, vol. 70, pp. 5639–5651, 2022.

[16] X.-W. Chang and Y. Guo, "Huber's M-estimation in relative GPS positioning: Computational aspects," *J. Geodesy*, vol. 79, nos. 6–7, pp. 351–362, Aug. 2005.

[17] J. L. Hodges and E. L. Lehmann, "Estimates of location based on rank tests," *Ann. Math. Statist.*, vol. 34, no. 2, pp. 598–611, Jun. 1963.

[18] I. Guvenc, C.-C. Chong, and F. Watanabe, "NLOS identification and mitigation for UWB localization systems," in *Proc. IEEE Wireless Commun. Netw. Conf.*, Mar. 2007, pp. 1571–1576.

[19] Y. T. Chan, W. Y. Tsui, H. C. So, and P.-C. Ching, "Time-of-Arrival based localization under NLOS conditions," *IEEE Trans. Veh. Technol.*, vol. 55, no. 1, pp. 17–24, Jan. 2006.

[20] C.-H. Park and J.-H. Chang, "Robust time-of-arrival source localization employing error covariance of sample mean and sample median in line-of-sight/non-line-of-sight mixture environments," *EURASIP J. Adv. Signal Process.*, vol. 2016, no. 1, p. 89, Dec. 2016.

[21] S. Gezici, H. Kobayashi, and H. V. Poor, "Nonparametric nonline-of-sight identification," in *Proc. IEEE 58th Veh. Technol. Conf.*, Orlando, FL, USA, Mar. 2003, pp. 2544–2548.

[22] F. Yin, C. Fritsche, F. Gustafsson, and A. M. Zoubir, "EM- and JMAP-ML based joint estimation algorithms for robust wireless geolocation in mixed LOS/NLOS environments," *IEEE Trans. Signal Process.*, vol. 62, no. 1, pp. 168–182, Jan. 2014.

[23] Y. Feng, C. Fritsche, F. Gustafsson, and A. M. Zoubir, "TOA-based robust wireless geolocation and Cramér–Rao lower bound analysis in harsh LOS/NLOS environments," *IEEE Trans. Signal Process.*, vol. 61, no. 9, pp. 168–182, May 2013.

[24] F. Gustafsson and F. Gunnarsson, "Mobile positioning using wireless networks," *IEEE Signal Process. Mag.*, vol. 22, no. 4, pp. 41–53, Jul. 2005.

[25] U. Hammes, E. Wolsztynski, and A. M. Zoubir, "Robust tracking and geolocation for wireless networks in NLOS environments," *IEEE J. Sel. Topics Signal Process.*, vol. 3, no. 5, pp. 889–901, Oct. 2009.

[26] B. Chen, X. Liu, H. Zhao, and J. C. Principe, "Maximum correntropy Kalman filter," *Automatica*, vol. 76, pp. 70–77, Feb. 2017.

[27] S. Fakoorian, R. Izanloo, A. Shamshirgaran, and D. Simon, "Maximum correntropy criterion Kalman filter with adaptive kernel size," in *Proc. IEEE Nat. Aerosp. Electron. Conf. (NAECON)*, Jul. 2019, pp. 581–584.

[28] X. Liu, H. Qu, J. Zhao, P. Yue, and M. Wang, "Maximum correntropy unscented Kalman filter for spacecraft relative state estimation," *Sensors*, 16, pp. 1–16, Sep. 2016.

[29] Y. Huang, Y. Zhang, N. Li, Z. Wu, and J. A. Chambers, "A novel robust student's t-based Kalman filter," *IEEE Trans. Aerosp. Electron. Syst.*, vol. 53, no. 3, pp. 1545–1554, Jun. 2017.

[30] Y. Huang, Y. Zhang, Y. Zhao, and J. A. Chambers, "A novel robust Gaussian–student's t mixture distribution based Kalman filter," *IEEE Trans. Signal Process.*, vol. 67, no. 13, pp. 3606–3620, Jul. 2019.

[31] Y. Huang, Y. Zhang, Y. Zhao, P. Shi, and J. A. Chambers, "A novel outlier-robust Kalman filtering framework based on statistical similarity measure," *IEEE Trans. Autom. Control*, vol. 66, no. 6, pp. 2677–2692, Jun. 2021.

[32] A. Coluccia and F. Ricciato, "RSS-based localization via Bayesian ranging and iterative least squares positioning," *IEEE Commun. Lett.*, vol. 18, no. 5, pp. 873–876, May 2014.

[33] Y. Hu and G. Leus, "Robust differential received signal strength-based localization," *IEEE Trans. Signal Process.*, vol. 65, no. 12, pp. 3261–3276, Jun. 2017.

[34] X. Guo, L. Chu, and X. Sun, "Accurate localization of multiple sources using semidefinite programming based on incomplete range matrix," *IEEE Sensors J.*, vol. 16, no. 13, pp. 5319–5324, Jul. 2016.

[35] C. Park and J. Chang, "Robust localization based on non-parametric kernel technique," *Electron. Lett.*, vol. 58, no. 22, pp. 850–852, Oct. 2022.

[36] H. Mehrabian and R. Ravanmehr, "Sensor fusion for indoor positioning system through improved RSSI and PDR methods," *Future Gener. Comput. Syst.*, vol. 138, pp. 254–269, Jan. 2023.

[37] J. Bi, M. Zhao, G. Yao, H. Cao, Y. Feng, H. Jiang, and D. Chai, "PSOSVR-Pos: WiFi indoor positioning using SVR optimized by PSO," *Expert Syst. Appl.*, vol. 222, Jul. 2023, Art. no. 119778.

[38] C. Zhao, A. Song, Y. Zhu, S. Jiang, F. Liao, and Y. Du, "Data-driven indoor positioning correction for infrastructure-enabled autonomous driving systems: A lifelong framework," *IEEE Trans. Intell. Transp. Syst.*, vol. 24, no. 4, pp. 3908–3921, Apr. 2023.

[39] B. E. Hansen, "Autoregressive conditional density estimation," *Intern. Econ. Rev.*, vol. 35, no. 3, pp. 705–730, Aug. 1994.

[40] H. Nurminen, T. Ardeshiri, R. Piché, and F. Gustafsson, "Robust inference for state-space models with skewed measurement noise," *IEEE Signal Process. Lett.*, vol. 22, no. 11, pp. 1898–1902, Nov. 2015.

[41] G. Miraglia, K. N. Maleki, and L. R. Hook, "Comparison of two sensor data fusion methods in a tightly coupled UWB/IMU 3-D localization system," in *Proc. Int. Conf. Eng., Technol. Innov. (ICE/ITMC)*, Jun. 2017, pp. 611–618.

[42] P. Müller, J. A. del Peral-Rosado, R. Piché, and G. Seco-Granados, "Statistical trilateration with Skew-t distributed errors in LTE networks," *IEEE Trans. Wireless Commun.*, vol. 15, no. 10, pp. 7114–7127, Oct. 2016.

[43] W. Xiong, C. Schindelhauer, H. C. So, J. Bordoy, A. Gabbrielli, and J. Liang, "TDOA-based localization with NLOS mitigation via robust model transformation and neurodynamic optimization," *Signal Process.*, vol. 178, pp. 1–10, Jan. 2021.
[44] K. Radnosrati, G. Hendeby, and F. Gustafsson, "Exploring positive noise in estimation theory," *IEEE Trans. Signal Process.*, vol. 68, pp. 3590–3602, 2020.
[45] C. E. O'Lone, H. S. Dhillon, and R. M. Buehrer, "Characterizing the first-arriving multipath component in 5G millimeter wave networks: TOA, AOA, and non-line-of-sight bias," *IEEE Trans. Wireless Commun.*, vol. 21, no. 3, pp. 1602–1620, Mar. 2022.
[46] Y. Xiong, N. Wu, Y. Shen, and M. Z. Win, "Cooperative localization in massive networks," *IEEE Trans. Inf. Theory*, vol. 68, no. 2, pp. 1237–1258, Feb. 2022.
[47] Y. Xiong, N. Wu, Y. Shen, and M. Z. Win, "Cooperative network synchronization: Asymptotic analysis," *IEEE Trans. Signal Process.*, vol. 66, no. 3, pp. 757–772, Feb. 2018.
[48] W. Yuan, N. Wu, Q. Guo, X. Huang, Y. Li, and L. Hanzo, "TOA-based passive localization constructed over factor graphs: A unified framework," *IEEE Trans. Commun.*, vol. 67, no. 10, pp. 6952–6965, Oct. 2019.
[49] L. L. Scharf, *Statistical Signal Processing: Detection, Estimation, and Time Series Analysis*, 1st ed. London, U.K.: Pearson, 1991.
[50] S. Manikandan, "Measures of central tendency: Median and mode," *J. Pharmacol. Pharmacotherapeutics*, vol. 2, no. 3, pp. 214–215, Sep. 2011.
[51] S. M. Kay, *Fundamentals of Statistical Signal Processing: Detection Theory*, vol. 2. Upper Saddle River, NJ, USA: Prentice-Hall, 1998.
[52] B. W. Silverman, *Density Estimation for Statistics and Data Analysis*. Boca Raton, FL, USA: CRC Press, 1986.
[53] L. Wasserman, *All of Statistics: A Concise Course in Statistical Inference*. Cham, Switzerland: Springer, 2010.
[54] C. Park and J. Chang, "WLS localization using skipped filter, Hampel filter, bootstrapping and Gaussian mixture EM in LOS/NLOS conditions," *IEEE Access*, vol. 7, pp. 35919–35928, 2019.
[55] K. Bregar and M. Mohorcic, "Improving indoor localization using convolutional neural networks on computationally restricted devices," *IEEE Access*, vol. 6, pp. 17429–17441, 2018.

CHEE-HYUN PARK received the Ph.D. degree in electronics and computer engineering from Sungkyunkwan University, Suwon, South Korea, in 2011. From April 2011 to August 2012, he was with the University of Wisconsin-Madison, Madison, WI, USA, as a Postdoctoral Fellow. Currently, he is a Research Professor with Hanyang University, Seoul, South Korea. His research interests include signal processing, statistics, source localization, and machine learning.

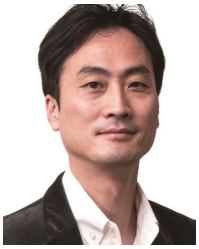

JOON-HYUK CHANG (Senior Member, IEEE) received the B.S. degree in electronics engineering from Kyungpook National University, Daegu, South Korea, in 1998, and the M.S. and Ph.D. degrees in electrical engineering from Seoul National University, South Korea, in 2000 and 2004, respectively. From 2000 to 2005, he was with Netdus Corporation, Seoul, as a Chief Engineer. From 2004 to 2005, he held a postdoctoral research position with the University of California at Santa Barbara, Santa Barbara, where he was involved in adaptive signal processing and audio coding. In 2005, he joined the Korea Institute of Science and Technology, Seoul, as a Research Scientist, where he was involved in speech recognition. From 2005 to 2011, he was an Assistant Professor with the School of Electronic Engineering, Inha University, Incheon, South Korea. He is currently a Full Professor with the School of Electronic Engineering, Hanyang University, Seoul, South Korea. His research interests include speech coding, speech enhancement, speech recognition, audio coding, and adaptive signal processing. He was a recipient of the IEEE/IEEK IT Young Engineer, in 2011. He is serving as the Editor-in-Chief for the Signal Processing Society of the IEEK.